



Effect of glycol-based coolants on the suppression and recovery of platinum fuel cell electrocatalysts

Yannick Garsany ^{a,c,*}, Sreya Dutta ^b, Karen E. Swider-Lyons ^c

^a Excat Inc., Springfield, VA 22151, USA

^b Dynalene Inc., Whitehall, PA 18052, USA

^c US Naval Research Laboratory, Washington, DC 20375, USA

HIGHLIGHTS

- ▶ Suppression and recovery of Pt/VC in glycol-based coolant formulations was studied.
- ▶ Glycol/water mixture causes loss of Pt ECSA and lowers ORR activity.
- ▶ Full recovery is achieved by transfer of poisoned electrode to clean electrolyte.
- ▶ Addition of surfactant to the coolant formulation does not affect the Pt/VC electrocatalysts.
- ▶ Azole corrosion inhibitors cause irreversible losses to the available Pt ECSA.

ARTICLE INFO

Article history:

Received 6 March 2012

Received in revised form

30 May 2012

Accepted 14 June 2012

Available online 23 June 2012

Keywords:

Pt/VC electrocatalysts

Fuel cells

PEMFCs

ORR

RDE

ABSTRACT

We use cyclic and rotating disk electrode voltammetry to study glycol-based coolant formulations to show that individual constituents have either negligible or significant poisoning effects on the nanoscale Pt/carbon catalysts used in proton exchange membrane fuel cells. The base fluid in all these coolants is glycol (1, 3 propanediol), commercially available in a BioGlycol coolant formulation with an ethoxylated nonylphenol surfactant, and azole- and polyol-based non-ionic corrosion inhibitors. Exposure of a Pt/Vulcan carbon electrode to glycol-water or glycol-water-surfactant mixtures causes the loss of Pt electrochemical surface area (ECSA), but the Pt ECSA is fully recovered in clean electrolyte. Only mixtures with the azole corrosion inhibitor cause irreversible losses to the Pt ECSA and oxygen reduction reaction (ORR) activity. The Pt ECSA and ORR activity can only be recovered to within 70% of its initial values after aggressive voltammetric cycling to 1.50 V after azole poisoning. When poisoned with a glycol mixture containing the polyol corrosion inhibitor instead, the Pt ECSA and ORR activity is completely recovered by exposure to a clean electrolyte. The results suggest that prior to incorporation in a fuel cell, voltammetric evaluation of the constituents of coolant formulations is worthwhile.

© 2012 Elsevier B.V. All rights reserved.

1. Introduction

Proton exchange membrane fuel cells (PEMFCs) are about 50% efficient for the conversion of hydrogen energy to electricity. The remaining inefficiencies produce waste heat that must be rejected to keep the PEMFC system at its optimal temperature, near 60–80 °C. The common methods for heat rejection are air-cooling, evaporative cooling of the liquid H₂O, or dissipation of the heat into a coolant loop system with a high-surface-area radiator.

A coolant loop with a radiator can be the most effective means to reject heat in a volume- and weight-effective manner over a wide range of power levels. In a multi-cell stack, the coolant is typically flowed through each cell to the radiator to keep uniform temperature with each coolant flow field isolated from the electrochemical compartments of each cell. If the coolant, which is typically glycol based [1–3], enters the electrochemical compartments of the cell it can pose a poisoning risk to the fuel cell platinum catalysts and cause a decrease in fuel cell performance. The coolant can come in contact with the Pt if the cell compartments are not sealed properly, or there are leaks through porous materials.

In principle, contact of the electrocatalysts with glycols should pose no risk to fuel cells, as such organic compounds oxidize at Pt electrodes [4–10]. Ethylene glycol has even been studied as a direct

* Corresponding author. US Naval Research Laboratory, Chemistry Division, 4555 Overlook Avenue, SW, Washington, DC 20375, USA. Tel.: +1 202 404 1825; fax: +1 202 404 8119.

E-mail address: yannick.garsany.ctr.fr@nrl.navy.mil (Y. Garsany).

fuel for electro-oxidation in fuel cells [11]. However, commercial coolants contain certain additives that can poison platinum-based electrocatalyst.

We report here the extent to which standard carbon-supported nanoscale Pt electrocatalysts are poisoned when they come in contact with coolant materials, and, more importantly, how the Pt performance can be recovered after poisoning. Several formulations of the fuel cell coolants were provided by Dynalene Inc, and we studied the poisoning effects of these coolant constituents on standard, commercial nanoscale platinum on Vulcan carbon electrocatalyst (Pt/VC). Cyclic voltammetric (CV) analysis was used for evaluation of the Pt electrochemical surface area (ECSA) and rotating disk electrode (RDE) methodology was applied for measurement of the oxygen reduction reaction (ORR) activity. In situ CV is considered to be an efficient and convenient method for the removal of adsorbed poisoning species such as SO_2 , H_2S , CO on Pt surface [12–15]. In the present case, we adapt CV methods that we have developed to study cathode poisoning with SO_2 and have been verified in studies of membrane electrode assemblies [14–17]. We have shown that the performance of SO_2 -poisoned Pt/VC working electrodes can be completely recovered by cycling the Pt/VC (and $\text{Pt}_3\text{Co}/\text{VC}$) working electrodes to 1.50 V, where the SO_2 is oxidized to sulfate (SO_4^{2-}) [12,13,15]. The charged SO_4^{2-} species are then desorbed when the Pt/VC working electrode is brought to low potentials (0.05 V) where the Pt loses its charge and the SO_4^{2-} can be desorbed [12,13,15]. The SO_2 can be completely removed over multiple cycles as it is oxidized to sulfate and desorbed, making more Pt sites available. This cycling process has been reduced to a practical method for a SO_2 -poisoned membrane electrode assembly cathode [17]. The cell is switched from normal H_2 /air operation to H_2/N_2 by electrochemically consuming oxygen in air. The cell cathode potential is then cycled from 0.09 V to 1.10 V vs. the anode potential to restore 97% of the initial Pt electrochemical surface area (ECSA). Further by using this in situ inert atmosphere cycling method, the polarizations curves of the poisoned membrane electrode assembly cathode returns to their original performance in less than 3 min.

In this paper, we determine the Pt ECSA of a clean Pt/VC electrocatalyst by CV method using a standard protocol of cycling the Pt/VC working electrode between 0.05 V and 1.20 V vs. RHE in N_2 -purged 0.10 M HClO_4 . The Pt/VC working electrode is then transferred to an electrolyte poisoned with the coolant constituents, and cycled using the standard cycling protocol, and then characterized again in a clean N_2 -purged 0.10 M HClO_4 electrolyte using the standard CV protocol plus examined in and for its oxygen reduction reaction (ORR) activity in O_2 -purged 0.10 M HClO_4 electrolyte. In the presence of more aggressive poisons, we cycle to 1.50 V, which has proven successful for SO_2 contamination. Based on this methodology, we provide a method to screen fuel cell coolant constituent materials for the reversibility of their poisoning interaction with Pt/VC.

2. Experimental

2.1. Electrode preparation

All poisoning studies were carried out on a commercially available catalyst comprising 19.7 wt % Pt supported on Vulcan carbon XC-72 (Pt/VC, E-TEK, currently BASF). For the RDE experiments, an ink of Pt/VC was prepared as described elsewhere [12,13,18,19], and this was cast on a glassy carbon electrode ($\varnothing = 5 \text{ mm}$, $A = 0.196 \text{ cm}^2$, Pine Instruments) by rotational drying at 700 rpm as described in reference [19]. The electrode Pt loading was kept close to $20 \mu\text{g}_{\text{Pt}} \text{ cm}^{-2}$ (geometric).

2.2. Coolant materials

The glycol-based fluid in all these coolants was 1, 3 propanediol, commercially available as BioGlycol (Dynalene, Whitehall PA). The surfactant was an ethoxylated nonylphenol. The non-ionic corrosion inhibitors comprised azoles (five-membered nitrogen heterocyclic ring compounds containing at least one other non-carbon atom of either nitrogen, sulfur, or oxygen) and polyols (alcohol containing multiple hydroxyl groups). Hereafter, these are called the azole and polyol inhibitors. The polyol-type is highly compatible with aluminum. Nanopure water (18 MΩ cm, Barnstead nanopure) was used as a diluent.

Five different coolant mixtures were made from the materials above for electrochemical evaluation with Pt/VC, and their formulation description are listed in Table 1.

2.3. Electrochemical measurements

All electrochemical measurements were carried out in standard three-electrode electrochemical glass cell maintained at a temperature of 30 °C, as described in reference [18]. The 0.10 M HClO_4 working electrolyte was prepared from double distilled HClO_4 (GFS Chemicals) and nanopure water (18 MΩ cm, Barnstead nanopure). Ultra high purity nitrogen (N_2) and oxygen (O_2) were employed (99.999% – Alphagaz 2, Air Liquide). A platinum mesh was used as the counter electrode and the reference electrode was an in-house constructed reversible hydrogen electrode (RHE) using a bridge containing the same concentration of electrolyte used in the experiment (0.10 M HClO_4) [18]. The working electrode was a glassy carbon substrate ($\varnothing = 5 \text{ mm}$) on which electrocatalyst ink aliquots were deposited. CV and ORR polarization curve measurements were carried out using an Autolab bi-potentiostat (PGSTAT30) and rotating disk electrode set-up (AFMSRX ring-disk rotator, Pine Instruments).

Fig. 1 presents the experimental procedure developed to study the effect of the coolant containing glycol/water, as is and with the addition of the surfactant and/or corrosion inhibitor, on the electrochemical characteristics of the Pt/VC electrocatalyst. Two three-electrode electrochemical glass cells were used, the first was kept clean and the second was used for contamination experiments. For a typical experiment, a Pt/VC working electrode was first conditioned in a “clean cell” by potential cycling between 0.0 V and 1.40 V vs. RHE for 100 cycles at a scan rate of 500 mV s⁻¹. The baseline CV (e.g., initial CV) was taken from the third cycle after cycling between 0.05 V and 1.20 V vs. RHE at a scan rate 50 mV s⁻¹.

The second cells, or “contamination cells”, were prepared by de-aerating 100 mL of 0.10 M HClO_4 electrolyte for 25 min with ultra high purity N_2 , and then adding 1 mL of the aforementioned coolant (with different variation of the constituents). The solution was continuously homogenized by N_2 bubbling and stirring. The conditioned Pt/VC working electrode was then placed in the contamination cell, and CVs were performed in the midst of the

Table 1
Selected coolants under evaluation.

Evaluated coolant item number	Description
Coolant #1	Glycol (1,3 propanediol)/water/surfactant/azole + polyol-based corrosion inhibitors
Coolant #2	Glycol/water
Coolant #3	Glycol/water/surfactant
Coolant #4	Glycol/water/surfactant/azole-based corrosion inhibitor
Coolant #5	Glycol/water/surfactant/polyol-based corrosion inhibitor

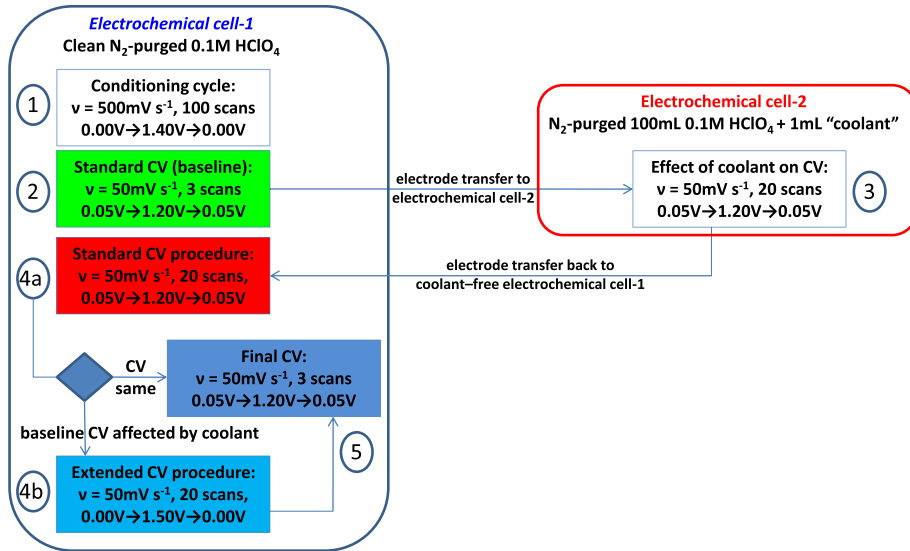


Fig. 1. Schematic of the experimental procedure designs to study the effect of the glycol-based coolant (or its constituents) on the cyclic voltammetric (CV) characteristics of Pt/VC electrocatalysts.

coolant material by cycling the Pt/VC working electrode potential between 0.05 V and 1.20 V at a scan rate of 50 mV s^{-1} for 20 cycles.

The poisoned Pt/VC working electrode was then withdrawn from the contamination cell covered with a droplet of the contaminated electrolyte, rinsed well with nanopure water, and then re-introduced into the clean electrochemical cell. Electrochemical cycling was then performed using the standard CV procedure. The poisoned Pt/VC working electrode was cycled between 0.05 V and 1.20 V vs. RHE at a scan rate 50 mV s^{-1} for 20 cycles. The CVs obtained using this standard CV procedure were then compared to the initial CV measured for the working Pt/VC electrode prior to the poisoning step. If the CVs recorded using the standard CV procedure differed significantly from the initial CV, an extended CV procedure was performed by cycling the poisoned Pt/VC working electrode between 0.00 V and 1.50 V vs. RHE at a scan rate of 50 mV s^{-1} for 20 cycles. This extended CV procedure step was implemented essentially as a cleaning step to remove any absorbed contaminants species from the poisoned Pt/VC working electrode surface [12,13,15]. A final series of CVs were then performed by cycling the working electrode potential between 0.05 V and 1.20 V at 50 mV s^{-1} for 3 cycles in order to compare the initial

Pt ECSA to the final Pt ECSA (i.e. Pt ECSA obtained after the extended CV procedure).

Fig. 2 illustrates the two experimental methods developed to study the effect of different formulation of the glycol-based coolant on the ORR. In method A, the clean electrochemical cell was used for all ORR polarization curve measurements in O_2 -saturated 0.10 M HClO_4 electrolyte. To obtain the initial ORR polarization curve, the Pt/VC working electrode was rotated at 1600 rpm and cycled between 1.03 V and 0.05 V vs. RHE at a scan rate of 20 mV s^{-1} for 3 cycles, and a steady-state CV based on the third cycle was recorded for analysis (initial ORR). The Pt/VC working electrode was then transferred to the contaminated cell where it was cycled between 0.05 V and 1.20 V at a scan rate 50 mV s^{-1} for 20 cycles at a rotation rate of 1600 rpm. The poisoned Pt/VC working electrode was then withdrawn covered with a droplet of the contaminated electrolyte, rinsed well with nanopure water and then re-introduced into the clean cell where the ORR polarization curves were measured again by cycling between 1.03 V and 0.05 V vs. RHE at 20 mV s^{-1} and 1600 rpm for 20 cycles. If needed the effectiveness of the extended cycling procedure on the ORR recovery was also tested using the methods depicted in **Fig. 2**.

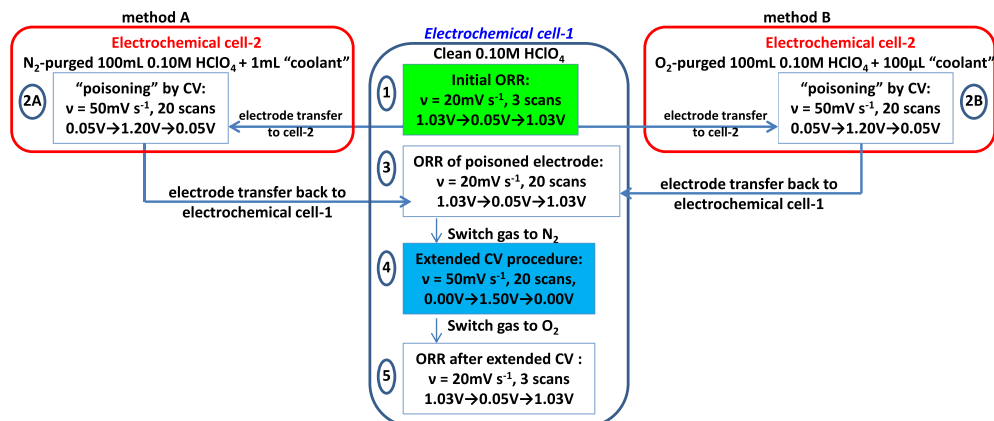


Fig. 2. Schematic of the experimental procedure designs to study the effect of the glycol-based coolant (or its constituents) on the ORR polarization curves of Pt/VC electrocatalysts.

In method B, after recording the initial ORR polarization curve in the clean electrochemical cell, the Pt/VC working electrode was transferred to the contaminated cell containing O₂-saturated 0.10 M HClO₄ + 100 μ L of different formulation of the glycol-based coolant. ORR polarization curves were measured again by cycling between 1.03 V and 0.05 V vs. RHE at 20 mV s⁻¹ and 1600 rpm for 20 cycles. The Pt/VC working electrode was then withdrawn from the contaminated cell, rinsed well with nanopure water and transferred to the clean electrochemical cell and ORR measurements were performed. Again, if needed the effectiveness of the extended cycling procedure on the ORR recovery was also tested using the methods depicted in Fig. 2.

3. Results and discussion

3.1. Effect of the glycol-based coolant on Pt/VC CV characteristics

The initial Pt/VC CV measured in a coolant-free N₂-purged 0.10 M HClO₄ in Fig. 3a exhibits the three separate potential regions representative of bulk platinum electrodes [20–22]: the hydrogen underpotential adsorption/desorption region (H_{upd}, 0.05 V \leq E \leq 0.40 V) is directly followed by the double layer potential region (ca. 0.40 V \leq E \leq 0.75 V), and then first by the reversible adsorption of OH, and finally by irreversible oxide formation. The CVs are a useful tool in the investigation of Pt poisoning because the area of the hydrogen region is directly proportional to the number of active sites available on the Pt surface, and the Pt-oxide region also has a unique signature on clean Pt. We chose to cycle between 0.05 V and 1.20 V to observe the full range of hydrogen adsorption/desorption and Pt oxide formation/stripping.

The CV of the Pt/VC working electrode changes significantly when cycled in the presence of the coolant#1 (i.e. glycol/water/surfactant/azole + polyol inhibitors), as shown by the series of 20 CVs in Fig. 3b. During the first positive sweep from 0.05 V to 1.20 V (CV-1, cyan curve), after the hydrogen potential region, a shoulder is first noticed at E = 0.50 V, then an anodic current peak (of about 2×10^{-4} A) at E = 0.90 V, the decrease part of which correspond to oxidation of the Pt surface. During the first reverse negative sweep from 1.20 V to 0.05 V (CV-1, cyan curve), an anodic current peak at around E = 0.70 V appears. As the number of CV cycles increases, the anodic peak current decrease progressively until CV-20 (black curve) when the CVs become stable.

Fig. 3c compares the initial CV measured for the Pt/VC working electrode in the clean electrochemical cell to CV-20 measured in the presence of coolant#1 in the contaminated electrochemical cell. Cycling the Pt/VC working electrode in the electrolyte containing coolant#1 causes a strong decrease in the electric charge associated with the hydrogen adsorption/desorption region (0.05 V–0.40 V) and the Pt-OH formation/reduction region is completely suppressed. These reductions are suggestive of adsorbed “poisoning species” on the surface of the Pt-metal nanoparticles blocking the sites for both hydrogen and OH adsorption. Further, a reversible surface process centered around E = 0.60 V is also clearly visible on CV-20 after cycling in the electrolyte containing the coolant#1 (i.e. glycol/water/surfactant/azole + polyol inhibitors).

The poisoning of the Pt/VC electrocatalyst by coolant#2 (glycol/water) vs. coolant#3 (glycol/water + surfactant) is compared in Fig. 4. Fig. 4a shows 20 CVs of a Pt/VC working electrode in a contaminated cell with coolant#2 and Fig. 4b shows parallel experiments of the Pt/VC exposed to coolant#3. The Pt/VC working electrode CVs look nearly identical in both the glycol/water and glycol/water + surfactant solutions. On the positive-going sweep, they both have a shoulder around E = 0.55 V before a large anodic

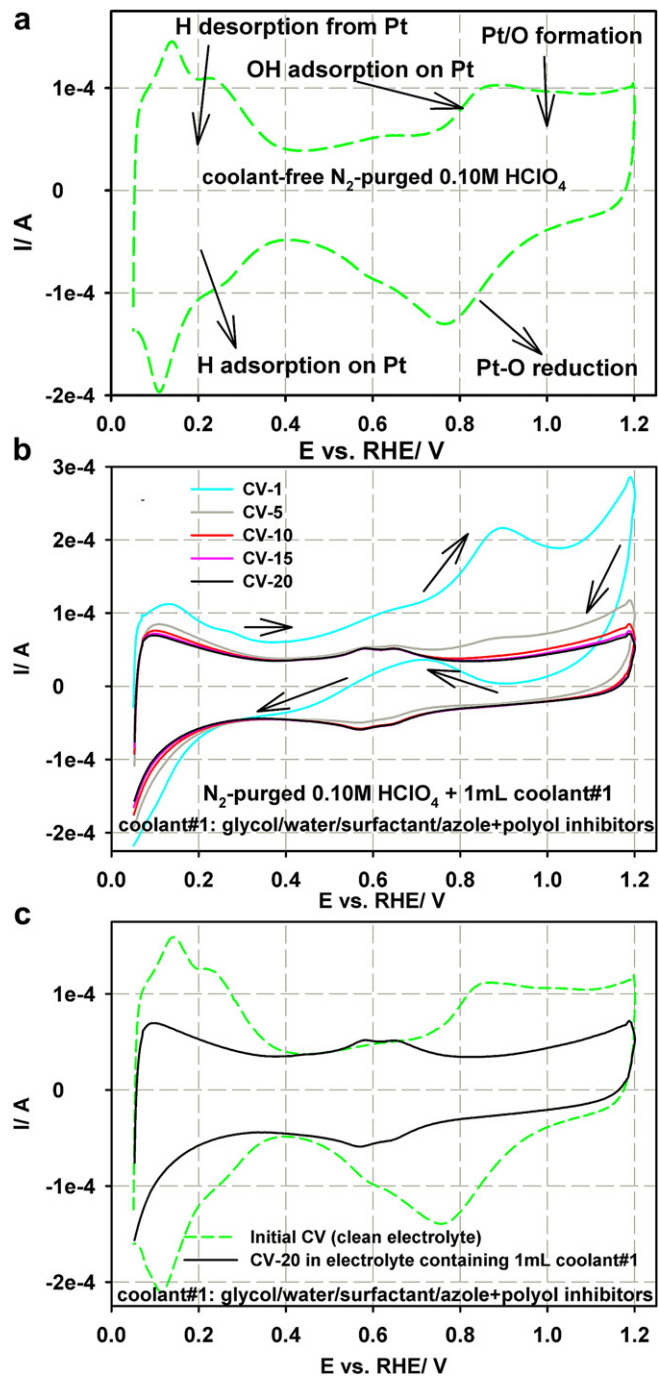


Fig. 3. a) Typical CV response obtained for a Pt/VC working electrode in clean N₂-purged 0.10 M HClO₄ electrolyte. b) Typical CV responses obtained for a Pt/VC working electrode in a N₂-purged 0.10 M HClO₄ electrolyte containing 1 mL of coolant#1. c) Comparison initial CV obtained for a Pt/VC working electrode in a clean N₂-purged 0.10 M HClO₄ electrolyte to CV-20 obtained for the same Pt/VC working electrode in N₂-purged 0.10 M HClO₄ electrolyte containing 1 mL of coolant#1. Conditions: scan rate of 50 mV s⁻¹ and cell temperature of 30 °C.

current peak centered around E = 0.90 V, and broad anodic peaks centered around E = 0.70 V on the negative sweeps. A decrease of the electric charge associated with hydrogen adsorption/desorption are also observed at $< E = 0.30$ V.

These results are consistent with glycol adsorption on the Pt/VC surface at low potentials and electro-oxidation of glycol above E = 0.60 V. The shape of these CV curves and the anodic current

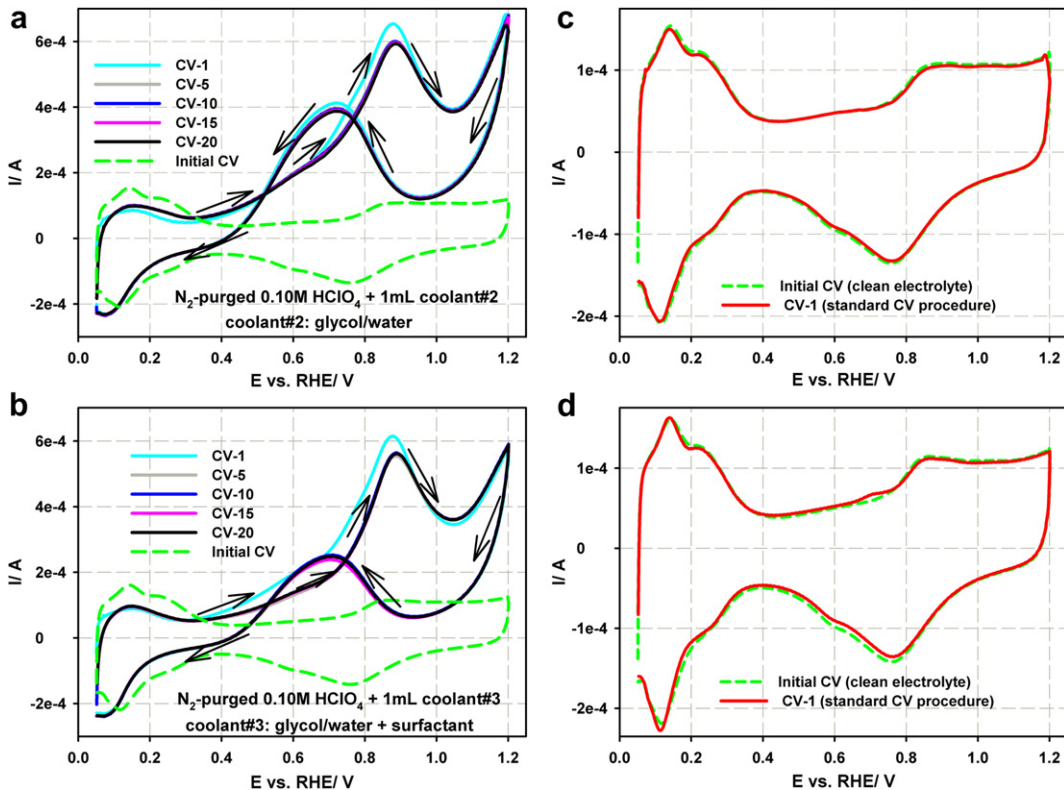


Fig. 4. a) Typical CV responses obtained for a Pt/VC working electrode in a N_2 -purged 0.10 M $HClO_4$ electrolyte containing 1 mL of coolant#2. The initial CV obtained for the same Pt/VC working electrode in a clean N_2 -purged 0.10 M $HClO_4$ electrolyte is added as a reference. b) Typical CV responses obtained for a Pt/VC working electrode in a N_2 -purged 0.10 M $HClO_4$ electrolyte containing 1 mL of coolant#3. The initial CV obtained for the same Pt/VC electrode in a clean N_2 -purged 0.10 M $HClO_4$ electrolyte is added as a reference. c) Comparison initial CV to CV-1 measured for the standard CV procedure (cycling between 0.05 V and 1.20 V for 20 cycles) for a poisoned Pt/VC working electrode in a clean N_2 -purged 0.10 M $HClO_4$. CV-1 (red curve) was performed after CV-20 (black curve) shown in Fig. 4a in the presence of 1 mL of coolant#2. d) Comparison initial CV to CV-1 for standard CV procedure for a poisoned Pt/VC working electrode in a clean N_2 -purged 0.10 M $HClO_4$ CV-1 (red curve) was performed after CV-20 (black curve) shown in Fig. 4b in the presence of 1 mL of coolant#3. Conditions: scan rate of 50 mV s⁻¹ and cell temperature of 30 °C. (For interpretation of the references to color in this figure legend, the reader is referred to the web version of this article.)

peak potentials are very comparable with previous reports for ethylene glycol electro-oxidation on Pt and Pt/VC [4–10]. There are only small changes during the potential scanning overtime. The first cycle (CV-1) exhibits slightly higher anodic current peaks in both positive and negative potential sweep scan. As the number of CV cycle increases (CV-1 to CV-5), the anodic current peaks decrease very slowly cycle by cycle. After five CV cycles, the voltammogram becomes relatively stable and the anodic current peaks remain unchanged but visible. This is clearly not the case for CV-20 measured in the electrolyte containing 1 mL of the coolant#1 (black curve on Fig. 3c): no anodic current peaks are visible on the voltammogram, the well known peaks of hydrogen adsorption/desorption and the peaks corresponding to the Pt/PtOx couple are completely suppressed indicating a severe poisoning of the Pt/VC working electrode by an unknown adsorbed species on the Pt nanoparticle surface.

After CV-20 obtained in Fig. 4a and b, the poisoned Pt/VC working electrodes were examined again using the standard CV procedure (cycling between 0.05 V and 1.20 V for 20 cycles, see Fig. 4c and d) in a clean N_2 -purged 0.10 M $HClO_4$ electrolyte. On the first CV cycle (red curves on Fig. 4c and d), the recorded CV for the poisoned Pt/VC working electrodes matches that of the initial Pt/VC CV in both the hydrogen adsorption/desorption and oxygen regions and shows full recovery of the Pt/VC electrocatalyst cyclic voltammetric features clearly implying that the products of the electro-oxidation of the glycol/water mixture does not lead to the poisoning of the Pt nanoparticle surface and that the addition of the

surfactant does not lead to further poisoning of the Pt/VC electrocatalyst surface. Further, this result indicates that the transfer of the poisoned Pt/VC working electrodes to a clean electrolyte is sufficient to remove any of the glycol/water/surfactant mixture from the Pt nanoparticle surface.

When the Pt/VC working electrode is contaminated with the glycol/water/surfactant + azole inhibitor mixture, the poisoning effect is severe. Fig. 5a shows a sequence of 20 CVs recorded for a Pt/VC working electrode contaminated with coolant#4 (i.e. glycol/water/surfactant mixture + azole inhibitor). The CVs of the Pt/VC working electrode poisoned by coolant#4 in Fig. 5a have the same features as for the Pt/VC working electrode poisoned by coolant#1 in Fig. 3b and c (see description above). Their final CVs (CV-20) are compared in Fig. 5b. The similarity of the CVs is striking, and clearly confirms that the azole inhibitor constituent in coolant#1 is responsible for the poisoning of the Pt/VC electrocatalyst.

Fig. 6 shows the results of the attempts to recover the performance of Pt/VC electrodes poisoned by coolant#1. Fig. 6a compares the first (CV-1) and last (CV-20) CVs recorded for the standard CV procedure (cycling between 0.05 V and 1.20 V) after the Pt/VC working electrode had undergone 20 CVs in the contamination cell with coolant#1. The initial CV recorded for the same Pt/VC working electrode in a clean electrolyte is also included for reference. The standard CV protocol does not result in any major recovery of the characteristic voltammetric features of the Pt metal nanoparticles. Again, for CV-1 the well known peaks

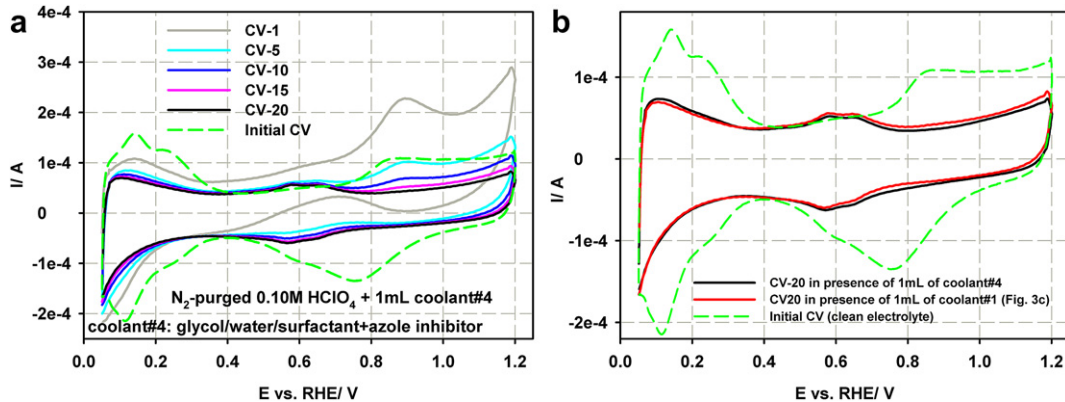


Fig. 5. a) Typical CV responses obtained for a Pt/VC working electrode in a N_2 -purged 0.10 M HClO_4 electrolyte containing 1 mL of coolant#4. b) Comparison CV-20 obtained for a Pt/VC working electrode in N_2 -purged 0.10 M HClO_4 electrolyte containing 1 mL of coolant#4 to CV-20 obtained for a Pt/VC working electrode in N_2 -purged 0.10 M HClO_4 electrolyte containing 1 mL of coolant#1. Conditions: scan rate of 50 mV s^{-1} and cell temperature of $30\text{ }^\circ\text{C}$. Initial CV obtained for the same Pt/VC working electrodes in a clean N_2 -purged 0.10 M HClO_4 electrolyte added as a reference on both Fig. 5a and b.

of hydrogen adsorption/desorption and the peaks corresponding to the Pt/PtO_x couple are completely suppressed indicating a severe poisoning of the Pt/VC working electrode. CV-20 is essentially identical to CV-1, clearly demonstrating that this standard potential cycling regime is not appropriate to remove the adsorbed poison species from the Pt nanoparticle surface after poisoning with coolant#1.

With the extended CV procedure (cycling between 0.00 V and 1.50 V), the CV characteristics of the Pt-metal nanoparticles do reappear on the Pt/VC working electrode poisoned in coolant#1 (Fig. 6b). The hydrogen adsorption/desorption and the peaks corresponding to the Pt/PtO_x couple increase slightly, indicating that some of the adsorbed contaminant is removed from the Pt surface using this extended CV procedure. Fig. 6c compares the initial

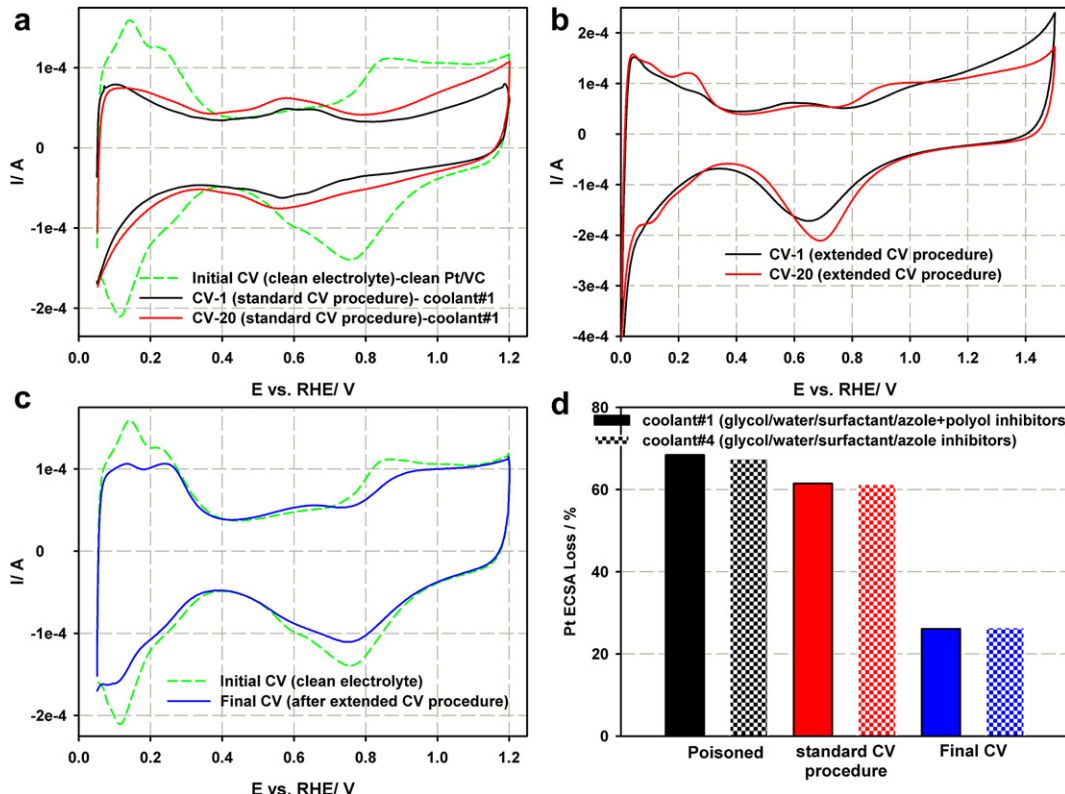


Fig. 6. a) Comparison CV-1 to CV-20 for standard CV procedure (cycling between 0.05 V and 1.20 V for 20 cycles) for a poisoned Pt/VC working electrode in a clean N_2 -purged 0.10 M HClO_4 . Standard CV procedure performed after CV-20 (black curve) shown in Fig. 5b in the presence of 1 mL of coolant#1. b) Comparison CV-1 to CV-20 for extended CV procedure (cycling between 0.00 V and 1.50 V for 20 cycles) for the poisoned Pt/VC working electrode in a clean N_2 -purged 0.10 M HClO_4 . c) Comparison initial CV obtained for the Pt/VC working electrode in a clean N_2 -purged 0.10 M HClO_4 electrolyte to final CV measured after CV-20 obtained for the extended CV procedure (red curve on Fig. 6b). d) Comparison percentage loss of Pt ECSA after poisoning of the Pt/VC working electrodes with coolant#1 and coolant#4. The Pt ECSA loss after standard (cycling between 0.05 V and 1.20 V) and extended CV procedures (cycling between 0.00 V and 1.50 V) is also included for comparison. (For interpretation of the references in color in this figure legend, the reader is referred to the web version of this article.)

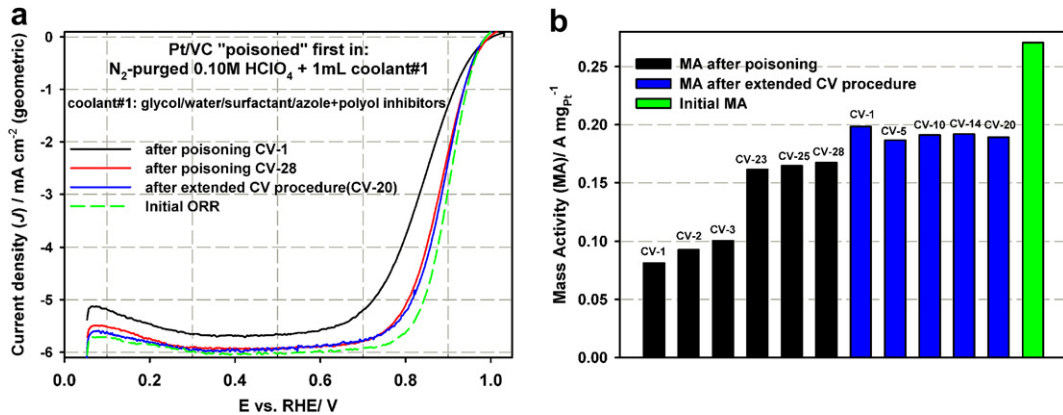


Fig. 7. a) Comparison ORR polarization curves measured for a Pt/VC working electrode immediately after running potential cycling in an electrolyte containing 1 mL of coolant#1 (CV-1, black curve and CV-28, red curve) to ORR polarization curve measured after extended CV procedure (CV-20, blue curve). The initial ORR polarization curve (obtained prior to “poisoning”) is shown for comparison. Conditions: scan rate of 20 mV s^{-1} , cell temperature of $30 \text{ }^\circ\text{C}$ and electrode rotation rate of 1600 rpm. b) MA calculated for the ORR polarization curves presented in Fig. 7a. (For interpretation of the references to color in this figure legend, the reader is referred to the web version of this article.)

(green dashed curve, same curve as shown on Fig. 3a) to the final CV (blue curve, obtained after CV-20 for extended CV procedure), and clearly shows that the extended CV procedure led to only partial recovery of the various surface-area dependent processes. The same results are obtained when the standard CV vs. the extended CV procedure are used to recover Pt/VC working electrodes poisoned by coolant#4.

The extent of the recovery of the Pt/VC working electrode was quantified by estimating the Pt ECSA in the working electrode calculated according to the methods in reference [18], from the amount of charge consumed during the hydrogen adsorption ($Q_{\text{H-adsorption}}$) after correction for double layer charging for the fresh and “poisoned” electrode and those recovered after the standard and extended CV procedures, respectively using Eq. (1):

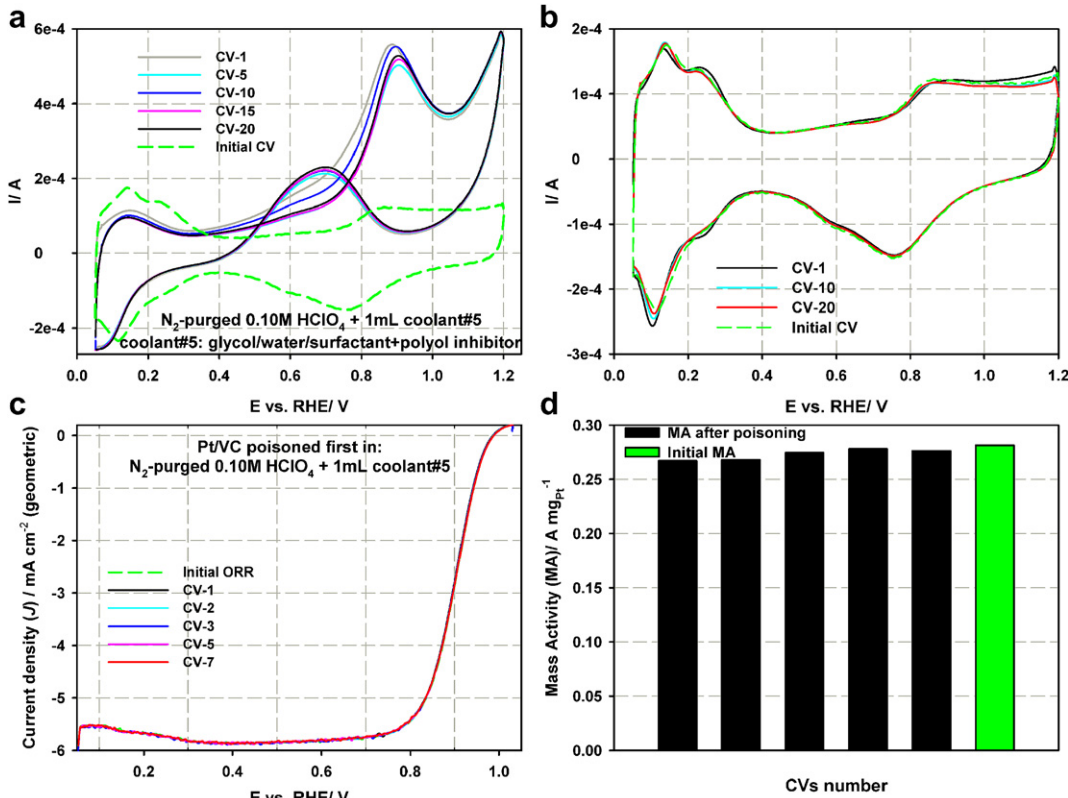


Fig. 8. a) Typical CV responses obtained for a Pt/VC working electrode in a N_2 -purged 0.10 M HClO_4 electrolyte containing 1 mL coolant#5. Initial CV obtained for the same Pt/VC working electrode in a clean N_2 -purged 0.10 M HClO_4 electrolyte added as a reference. b) Comparison initial CV to CV-1, CV-10 and CV-20 measured for the standard CV procedure (cycling between 0.05 V and 1.20 V for 20 cycles) for the poisoned Pt/VC working electrode in a clean N_2 -purged 0.10 M HClO_4 electrolyte. Standard CV procedure performed after CV-20 (black curve) shown in Fig. 8a in the presence of 1 mL of coolant#5. Conditions: scan rate of 50 mV s^{-1} and cell temperature of $30 \text{ }^\circ\text{C}$. c) Comparison CV-1 to CV-7 of ORR polarization curves measured for the same Pt/VC working electrode immediately after running CV-20 (black curve) shown in Fig. 8a in the presence of 1 mL of coolant#5. Conditions: scan rate of 20 mV s^{-1} , cell temperature of $30 \text{ }^\circ\text{C}$ and electrode rotation rate of 1600 rpm. d) MA calculated for the ORR polarization curves presented in Fig. 8c.

$$\text{ESCA}_{\text{Pt,cat}} \left(\text{m}^2 \text{g}_{\text{Pt}}^{-1} \right) = \left[\frac{Q_{\text{H-adsorption}}(\text{C})}{210 \mu\text{C} \text{cm}_{\text{Pt}}^{-2} L_{\text{Pt}}(\text{mg}_{\text{Pt}} \text{cm}^{-2}) A_{\text{g}}(\text{cm}^2)} \right] 10^5 \quad (1)$$

The charge of full coverage for clean polycrystalline Pt is $Q_{\text{H}} = 210 \mu\text{C} \text{cm}^{-2}$ and is used as the conversion factor. The Pt electrochemical surface area (ESCA_{Pt,cat}) is reported in $\text{m}^2 \text{g}_{\text{Pt}}^{-1}$; L_{Pt} is the working electrode Pt loading ($\text{mg}_{\text{Pt}} \text{cm}^{-2}$) and A_{g} (cm^2) is the geometric surface area of the glassy carbon electrode (i.e., 0.196 cm^2). The loss of Pt ECSA due to “adsorbed” contaminant is calculated using Eq. (2):

$$\text{ESCA}_{\text{loss}}(\%) = \left[\frac{(\text{ESCA}_{\text{initial}} - \text{ESCA}_{\text{final}})}{\text{ESCA}_{\text{initial}}} \right] \times 100 \quad (2)$$

where $\text{ESCA}_{\text{initial}}$ is the Pt ECSA obtained for the clean Pt/VC and $\text{ESCA}_{\text{final}}$ is the Pt ECSA obtained after the standard CV and extended CV procedures, respectively. The results are presented in Fig. 6d for Pt/VC working electrodes poisoned with coolant#1 (with azole and polyol inhibitors) and coolant#4 (with azole inhibitor), respectively. The initial Pt ECSA measured in a coolant-free electrolyte is $58 \text{ m}^2 \text{g}_{\text{Pt}}^{-1}$. After 20 CV cycles in the presence of coolant#1, the measured Pt ECSA drops by 68% to $16 \text{ m}^2 \text{g}_{\text{Pt}}^{-1}$. The standard CV protocol improves the Pt ECSA to only $23 \text{ m}^2 \text{g}_{\text{Pt}}^{-1}$, or 63% of the initial Pt ECSA remains loss. After applying the extended CV procedure, the measured Pt ECSA is equal to $43 \text{ m}^2 \text{g}_{\text{Pt}}^{-1}$, or is within 26% of the initial Pt ECSA indicating that the additional oxidation imposed by going up to 1.50 V helps to remove some of the coolant contaminants, but it is still insufficient to return the Pt/VC electrocatalyst to its initial state. Again, Fig. 6c clearly demonstrates that the azole inhibitor is responsible for the poisoning of the Pt/VC electrocatalyst as the Pt ECSA loss estimated for the Pt/VC working electrode poisoned in the N_2 -purged 0.10 M HClO_4 electrolyte containing 1 mL of coolant#4 (glycol/water/surfactant mixture + azole) matches pretty well with those estimated for the original glycol-based coolant (i.e. coolant#1, glycol/water/surfactant mixture/azole + polyol).

3.2. Effect of the glycol-based coolant on the ORR (method A)

The glycol-based coolant (i.e. coolant#1) also has significant impact on the oxygen reduction activity of the Pt/VC working electrode as presented in Fig. 7a. The initial ORR polarization curve (green dashed curve) recorded for the same Pt/VC working electrode in a clean O_2 -saturated 0.10 M HClO_4 electrolyte prior to the poisoning step is also shown as a reference.

The initial ORR polarization curve of the clean Pt/VC working electrode (green dashed curve) has a well defined diffusion-limiting current density plateau (J_{lim}) of -6 mA cm^{-2} geometric at $E = 0.10\text{--}0.80 \text{ V}$, followed by a region under mixed kinetic-diffusion control at $0.82 \text{ V} < E < 1.00 \text{ V}$. After cycling the Pt/VC working electrode in the electrolyte containing coolant#1 prior to the ORR measurements, the onset potential for the ORR shifts to lower potentials. On CV-1 (black curve), the ORR polarization curve measured for the poisoned Pt/VC working electrode shifts to lower current density and exhibits about 39 mV more overpotential at $J = -1.5 \text{ mA cm}^{-2}$ relative to initial ORR polarization curve (green dash curve on Fig. 7a). Further, the poisoning of the Pt/VC surface also results in a small decrease in the magnitude of the diffusion limiting current density plateau (J_{lim}) from -6 to $\sim -5.65 \text{ mA cm}^{-2}$. This decrease in J_{lim} could be attributed to either a decrease in the Pt ECSA or to a change in the selectivity of the ORR, i.e. the change of the oxygen reduction pathway from a 4e^- reduction mechanism (to form water) to a 2e^- reduction

mechanism (to form hydrogen peroxide) [12,13]. On successive scans, the onset potential for the ORR shifts towards more positive potentials, and the ORR potential at $J = -1.5 \text{ mA cm}^{-2}$ increases from $\sim 0.89 \text{ V}$ for CV-1 to 0.92 V for CV-28, coming within 10 mV of the potential measured for the clean Pt/VC working electrode (ca. the initial ORR curve). The value of the J_{lim} also increases with successive scans, nearly recovering by CV-28. Fig. 7a also shows that applying the extended CV procedure (cycling the Pt/VC working electrode between 0.00 V and 1.50 V to electrochemically clean the Pt surface) did not improve the ORR polarization curve significantly.

The catalytic activity of Pt/VC electrocatalyst for the ORR is best compared by its mass activity (MA) as calculated from the ORR polarization curves shown in Fig. 7a. The MA value is calculated using the mass transport-correction for thin-film RDEs normalization to the Pt-loading of the disk electrode [18], where the kinetic current, I_k , is taken from the value of the curve at $E=0.90 \text{ V}$ and the J_{lim} at $E = 0.50 \text{ V}$ vs. RHE. These Pt MAs are compared in Fig. 7b. The

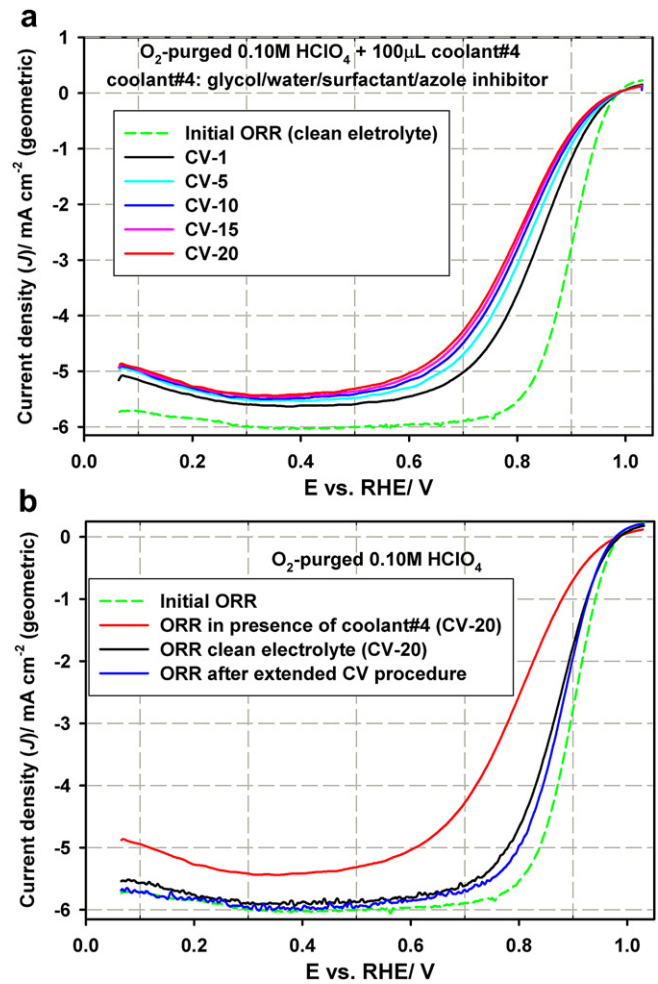


Fig. 9. a) Typical ORR polarization curves obtained for a Pt/VC working electrode in a O_2 -saturated 0.10 M HClO_4 electrolyte containing $100 \mu\text{L}$ of coolant#4. b) Comparison of the ORR polarization curve obtained in a 0.10 M HClO_4 electrolyte containing $100 \mu\text{L}$ of coolant#4 (red curve) to the ORR polarization curve obtained with the same poisoned Pt/VC working electrode in a clean electrolyte (black curve) and to ORR polarization curve obtained after running the extended CV procedure (blue curve). The initial ORR polarization curve obtained for the same Pt/VC working electrodes in a clean O_2 -purged 0.10 M HClO_4 electrolyte is added as a reference on both Fig. 9a and b. Conditions: scan rate of 20 mV s^{-1} , cell temperature of 30°C and electrode rotation rate of 1600 rpm . (For interpretation of the references to color in this figure legend, the reader is referred to the web version of this article.)

MA measured for the clean Pt/VC electrode is equal to $0.27 \text{ A mg}_{\text{Pt}}^{-1}$. After poisoning of the Pt/VC electrocatalyst, the MA measured for CV-1 is equal to $0.08 \text{ A mg}_{\text{Pt}}^{-1}$ or a 70% loss of the initial MA. Note that the MA loss calculated for CV-1 (i.e. 70%) is essentially identical to Pt ESCA loss calculated after the initial poisoning of the Pt/VC electrode (i.e. 68% see Fig. 6d), clearly indicating that Pt ECSA loss is the cause of the MA loss. As cycling progress (CV-1 to CV28), the MA increases from $0.08 \text{ A mg}_{\text{Pt}}^{-1}$ to about $0.17 \text{ A mg}_{\text{Pt}}^{-1}$. After implementing the extended CV procedure, the MA calculated for CV-20 is

only equal to $0.19 \text{ A mg}_{\text{Pt}}^{-1}$ or 70% of the initial MA is recovered. These results clearly indicate that even after cycling the poisoned Pt/VC working to 1.50 V, only a partial recovery of the initial MA is possible.

3.3. Effect of the non-ionic polyol corrosion inhibitor on Pt/VC

Based on the observation above that the azole inhibitor was causing irreversible Pt surface area loss and poor ORR activity of the

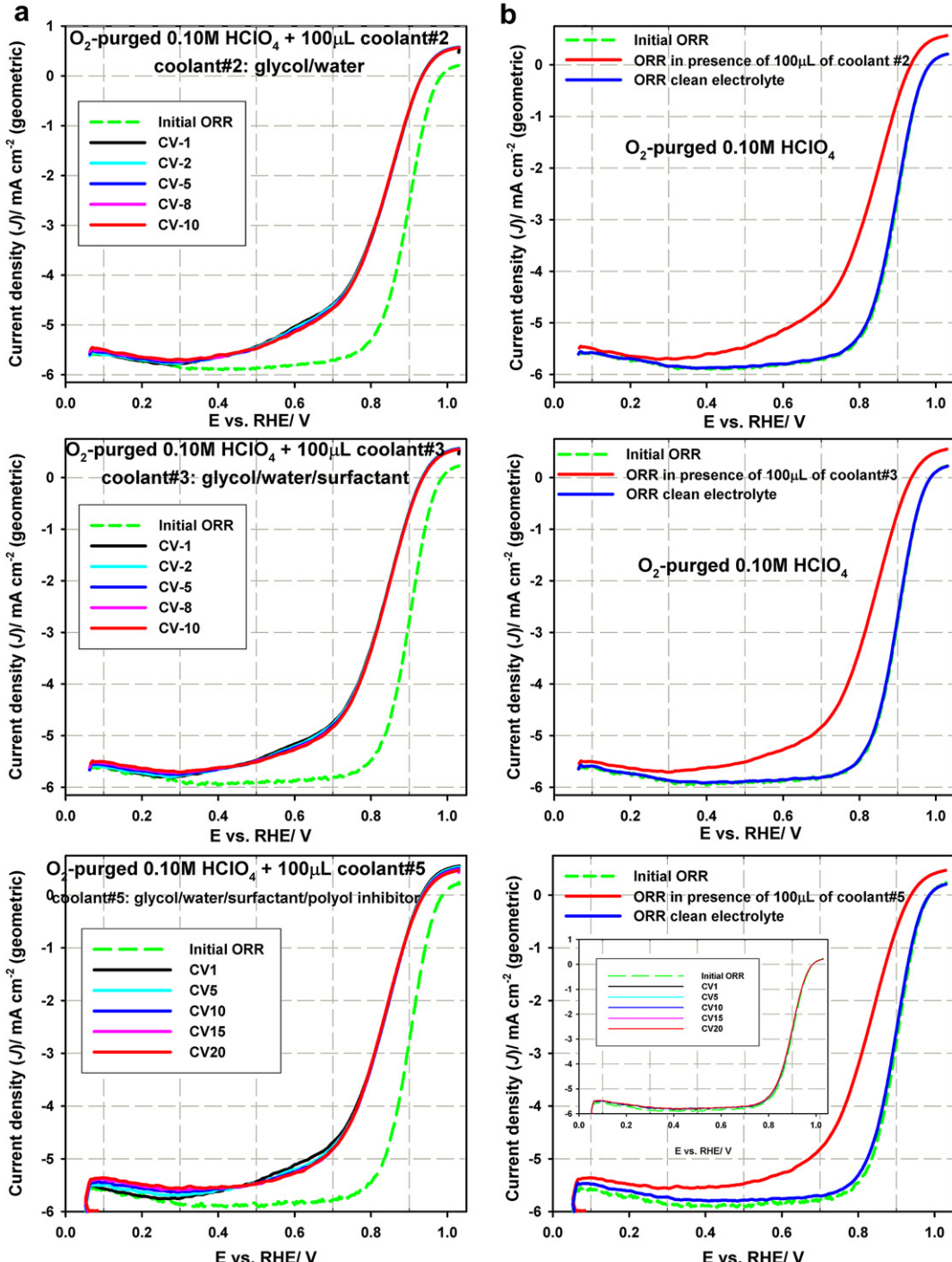


Fig. 10. a) Typical ORR polarization curves obtained for a Pt/VC working electrode in a O_2 -saturated 0.10 M HClO_4 electrolyte containing $100 \mu\text{L}$ of coolant#2, coolant#3 and coolant#5, respectively (left hand side). b) Comparison of the ORR polarization curves obtained in a 0.10 M HClO_4 electrolyte containing $100 \mu\text{L}$ of coolant#2, #3 and #5 (red curves) to the ORR polarization curve obtained with the same poisoned Pt/VC working electrode in a clean electrolyte (blue curves). Conditions: scan rate of 20 mV s^{-1} , cell temperature of 30°C and electrode rotation rate of 1600 rpm . (For interpretation of the references to color in this figure legend, the reader is referred to the web version of this article.)

Pt/VC catalysts, we examined another variation of the coolant formulation containing glycol/water/surfactant mixture + polyol inhibitor (i.e. coolant#5). We find that for the polyol corrosion inhibitor, there is now no irreversible poisoning effect.

Fig. 8a shows a sequence of 20 CV cycles recorded for a Pt/VC working electrode contaminated with coolant#5. The CVs of the Pt/VC working electrode poisoned with coolant#5 in Fig. 8a have the same features as for the Pt/VC working electrode poisoned by coolant#2 (i.e. glycol/water) in Fig. 4a. After five CV cycles, the voltammogram becomes relatively stable and the anodic current peaks remain unchanged but visible. In comparison, the original azole inhibitor is much more poisonous to the Pt/VC working electrode. Fig. 5a clearly shows that by CV-5 no anodic current peaks are visible on the voltammogram, the well known peaks of hydrogen adsorption/desorption and the peaks corresponding to the Pt/PtO_x couple are completely suppressed indicating a severe poisoning of the Pt/VC working electrode by the azole inhibitor.

The non poisonous effect of the polyol inhibitor is also obvious in the CVs measured using the standard cycling procedure (cycling between 0.05 V and 1.20 V for 20 cycles) which shows complete recovery of the characteristics of the Pt-metal nanoparticles (Fig. 8b). On the first CV cycle from 0.05 V up to 1.20 V vs. RHE, the CV of the poisoned Pt/VC working electrode matches that of baseline CV in both the hydrogen and oxygen regions and shows full recovery of the Pt/VC electrocatalyst voltammetric features, indicating that the presence of the polyol inhibitor does not lead to the irreversible poisoning of the Pt nanoparticle surface. Poisoning of the Pt/VC electrocatalyst with coolant#5 also has no significant impact on the oxygen reduction activity of the Pt/VC electrocatalyst as presented in Fig. 8c. The initial ORR polarization curve (green dash curve) recorded for the same Pt/VC working electrode in a clean O₂-saturated 0.10 M HClO₄ electrolyte prior to the poisoning step is shown as a reference. After poisoning with the coolant#5, the onset potential for the ORR remains the same. The MA measured for the clean Pt/VC working electrode is equal to 0.27 A mg_{Pt}⁻¹. After poisoning of the Pt/VC electrocatalyst with coolant#5, the MA measured for CV-1 is equal to 0.26 A mg_{Pt}⁻¹, compared to the 30% loss measured from azole inhibitor after cycling to 1.50 V.

3.4. ORR in the presence of the glycol-based coolant (method B)

Fig. 9a compares the initial ORR polarization curve (green dashed curve) obtained for a Pt/VC working electrode in a clean O₂-saturated 0.10 M HClO₄ electrolyte to the ORR polarization curves measured in a O₂-saturated 0.10 M HClO₄ electrolyte containing 100 μ L of coolant#4 (glycol/water/surfactant mixture + azole inhibitor). Fig. 9a clearly shows that addition of coolant#4 to the working electrolyte shifts the onset potential for the ORR to lower potentials. On CV-1 (black curve), the Pt/VC electrocatalyst exhibits about 60 mV more overpotential at $J = -1.5$ mA cm⁻² relative to the ORR polarization curve measured for the Pt/VC electrocatalyst in a coolant-free working electrolyte (green dashed curve). The poisoning of the Pt/VC electrocatalyst results in a decrease in the magnitude of the diffusion limiting current density plateau (J_{lim}) from -6 to ~ -5.5 mA cm⁻². On successive scans, the onset potential for the ORR shifts towards more negative potentials, and the ORR potential at $J = -1.5$ mA cm⁻² decreases from 0.87 V for CV-1 to 0.85 V for CV-20, 73 mV more negative than the potential measured for the Pt/VC working electrode in the clean electrolyte. The value of the J_{lim} also decreases with successive scans from ~ -5.5 mA cm⁻² for CV-1 (black curve) to ~ -5.3 mA cm⁻² for CV-20 (red curve). All these data suggest that the ORR efficiency of the Pt/VC working electrode deteriorates with cycling when coolant#4 is present in the working electrolyte. Further, when the Pt/VC working electrode is re-introduced to the coolant free O₂-saturated

0.10 M HClO₄ electrolyte, as shown in Fig. 9b, the initial ORR electrocatalytic activity is not fully recovered (black curve on Fig. 9b). Fig. 9b also shows that applying the extended CV procedure (cycling the Pt/VC working electrode between 0.0 V and 1.50 V in a N₂-purged 0.10 M HClO₄ electrolyte to electrochemically clean the Pt surface) did not improve the ORR polarization curve significantly. Again, the data strongly suggest to the irreversible poisoning of the Pt/VC electrocatalyst surface by coolant#4.

Fig. 10a (left hand side) compares the initial ORR polarization curve (green dashed curve) obtained for a Pt/VC working electrode in a clean O₂-saturated 0.10 M HClO₄ electrolyte to the ORR polarization curves measured in a O₂-saturated 0.10 M HClO₄ electrolyte containing 100 μ L of coolant#2, coolant#3 and coolant#5, respectively. Fig. 10a clearly shows that the ORR polarization curves measured in the presence of coolant #2, #3 and #5 are essentially identical. When these coolants are present in the working electrolyte, the ORR polarization curves measured for Pt/VC electrocatalyst exhibits about 60 mV more overpotential at $J = -1.5$ mA cm⁻² relative to initial ORR polarization curve measured in the coolant-free working electrolyte. On successive scans, there is no shift of the ORR onset potential and J_{lim} remains unchanged. The final CV (CV-10 or CV-20) is identical to CV-1. Further, when the Pt/VC working electrode is reintroduced to the coolant free O₂-saturated 0.10 M HClO₄ working electrolyte, as shown in Fig. 10b (right hand side), the Pt/VC electrocatalyst ORR catalytic activity is fully recovered. The recovery of ORR catalytic activity is achieved on the first scan from 1.03 V to 0.05 V as shown in the inset graph in Fig. 10b. These observations are different than for coolant#4, as shown on Fig. 9a and b, respectively. Again, this clearly indicates that the addition of the azole inhibitor to the glycol-based coolant has a harmful effect on the ORR catalytic activity of the Pt/VC electrocatalyst.

4. Conclusions

The glycol (1, 3 propandediol)/water based coolant with the surfactant and polyol corrosion inhibitor suppresses the activity of Pt/VC electrocatalysts, but can be recovered with exposure to clean electrolyte. Presence of surfactants in the coolant showed the same poisoning and reversible behavior as the aforementioned coolant itself. The biggest poisoning risk is posed by the azole-based non-ionic corrosion inhibitor added to coolant to prevent the corrosion of the metals in the coolant loop. Addition of the azole inhibitor causes irreversible loss to the Pt surface area and ORR activity. While effort should be made to protect Pt/VC from exposure to any coolant, any accidental exposure can be mitigated through the proper screening of the coolant constituents. The results also suggest that in a practical system, simply flushing the system with pure water (which would occur during operation) can be used to remove organic components of a coolant formulation, and work is underway in our laboratory to demonstrate this observation in a practical fuel cell system. Lastly the work suggests that voltammetric studies are a useful means for vetting whether foreign materials introduced into a fuel cell are poisonous or innocuous.

Acknowledgements

The authors are grateful to the Office of Naval Research for financial support of this project. We would like to thank Satish Mohapatra and Patrick McMullen (Dynalene Inc.) for useful discussions and providing the coolant materials.

References

- [1] S.C. Mohapatra, US. Pat. 7138199 B2, (2006).
- [2] S.C. Mohapatra, CA 2447174 C (2008).

- [3] S.C. Mohapatra, EP 1 416 563 B2, (2010).
- [4] F. Kadırgan, B. Beden, C. Lamy, J. Electroanal. Chem. 136 (1982) 119–138.
- [5] J.M. Orts, A. Fernandezvega, J.M. Feliu, A. Aldaz, J. Clavilier, J. Electroanal. Chem. 290 (1990) 119–133.
- [6] M.S. Ureña-Zanartu, C. Yanez, M. Paez, G. Reyes, J. Electroanal. Chem. 405 (1996) 159–167.
- [7] R.B. de Lima, V. Paganin, T. Iwasita, W. Vielstich, Electrochim. Acta 49 (2003) 85–91.
- [8] R.J. Behm, H. Wang, Z. Jusys, J. Electroanal. Chem. 595 (2006) 23–36.
- [9] R.J. Behm, H. Wang, Y. Zhao, Z. Jusys, J. Power Sources 155 (2006) 33–46.
- [10] Z. Jusys, H. Wang, R.J. Behm, J. Power Sources 154 (2006) 351–359.
- [11] V. Livshits, E. Peled, J. Power Sources 161 (2006) 1187–1191.
- [12] Y. Garsany, O.A. Baturina, K.E. Swider-Lyons, J. Electrochem. Soc. 154 (2007) B670–B675.
- [13] Y. Garsany, O.A. Baturina, K.E. Swider-Lyons, J. Electrochim. Soc. 156 (2009) B848–B855.
- [14] B.D. Gould, O.A. Baturina, K.E. Swider-Lyons, J. Power Sources 188 (2009) 89–95.
- [15] O.A. Baturina, B.D. Gould, Y. Garsany, K.E. Swider-Lyons, Electrochim. Acta 55 (2010) 6676–6686.
- [16] B. Gould, O.A. Baturina, Y. Garsany, K. Swider-Lyons, Abst. Papers Am. Chem. Soc. 238 (2009).
- [17] B.D. Gould, G. Bender, K. Bethune, S. Dorn, O.A. Baturina, R. Rocheleau, K.E. Swider-Lyons, J. Electrochim. Soc. 157 (2010) B1569–B1577.
- [18] Y. Garsany, O.A. Baturina, K.E. Swider-Lyons, S.S. Kocha, Anal. Chem. 82 (2010) 6321–6328.
- [19] Y. Garsany, I.S. Singer, K.E. Swider-Lyons, J. Electroanal. Chem. (2011) 396–406.
- [20] K. Franaszczuk, J. Sobkowski, J. Electroanal. Chem. 261 (1989) 223–227.
- [21] H.A. Gasteiger, N. Markovic, P.N. Ross, E.J. Cairns, J. Phys. Chem. 97 (1993) 12020–12029.
- [22] H.A. Gasteiger, N. Markovic, P.N. Ross, E.J. Cairns, J. Electrochim. Soc. 141 (1994) 1795–1803.